Bmp4 signaling is required for outflow-tract septation and branchial-arch artery remodeling

Wei Liu*, Jennifer Selever*, Degang Wang*, Mei-Fang Lu*, Kelvin A. Moses†, Robert J. Schwartz†, and James F. Martin*‡

*Alkek Institute of Biosciences and Technology, Texas A&M University System Health Science Center, 2121 Holcombe Boulevard, Houston, TX 77030; and †Department of Molecular and Cellular Biology, Baylor College of Medicine, Houston, TX 77030

Edited by Eric N. Olson, University of Texas Southwestern Medical Center, Dallas, TX, and approved January 30, 2004 (received for review December 18, 2003)

The *Bmp4* signaling molecule is expressed in ventral splanchnic and branchial-arch mesoderm and outflow-tract (OFT) myocardium, suggesting a role for *Bmp4* in OFT development. Inactivation of *Bmp4* in the caudal branchial arch and splanchnic mesoderm and OFT myocardium by using a conditional null allele of *Bmp4* and the *Nkx2.5^{cre} recombinase* allele resulted in abnormal morphogenesis of branchial-arch arteries (BAAs) and defective OFT septation. Expression of aortic-sac myocardial markers was reduced and expression of the *sm22^{LacZ}* transgene, a smooth-muscle marker, was attenuated in BAAs and conotruncus of *Nkx2.5^{cre}; Bmp4* conditional mutants. Moreover, we found tissue-specific functions for *Bmp4* in the regulation of cellular proliferation and apoptosis. We also demonstrate a strong genetic interaction between *Bmp4* and *Bmp7* in OFT development. Our findings uncover a previously uncharacterized function for *Bmp4* in vascular remodeling of the BAAs, and they show definitively that *Bmp4*, in cooperation with *Bmp7*, has a central role in OFT septation.

The vertebrate heart can be subdivided into inflow, outflow, and primitive-ventricular regions (1). The cardiac outflow tract (OFT), which develops from the anterior part of the linear heart tube, forms the right-sided conotruncal region after heart looping. Initially unseptated, the OFT divides into the pulmonary trunk (PT) and aorta, and it is critical for separation of postnatal pulmonary and systemic circulation. Congenital OFT malformations are common, making an understanding of the genetic pathways regulating OFT development an important goal in developmental biology and clinical medicine.

At defined areas of the OFT, endocardial cells undergo an epithelial to mesenchymal transformation (perhaps in response to a signal from overlying myocardium) and invade the intervening space to form the endocardial cushions. The cardiac neural crest also invades the forming aorto-pulmonary (AP) septum and OFT cushions (2). The OFT myocardium receives an additional input from splanchnic and branchial-arch mesoderm, the anterior or secondary heart field (SHF), which may be important for OFT lengthening and morphogenesis (3).

Bmp4 is a member of the *Bone morphogenetic protein* (*Bmp*) subclass of transforming growth factor type β (TGF-β)-signaling molecules (4). *Bmp4* expression in splanchnic and branchial-arch mesoderm (which contributes to OFT myocardium) and within the OFT myocardium itself suggests a role in OFT morphogenesis (ref. 5 and see below). Investigation of *Bmp4* function in cardiac development has been hampered by the early embryonic lethality of *Bmp4* null mutant embryos (6). Recent work analyzing an allele of the ubiquitously expressed *Bmp type 2 receptor* (*Bmpr2*), containing a partial ectodomain deletion, revealed defective proximal OFT septation in mouse embryos, providing insight into *Bmp* function in the OFT (7). However, because *Bmpr2* is broadly expressed, the developmental mechanisms responsible for the cushion defects remain unclear. Overexpression of *noggin* in chick embryos suggested that Bmp signaling is required for both migration of cardiac neural crest and proliferation of OFT mesenchyme (8). Moreover, inactivation of *Bmp4* in the heart by using a *cardiac troponin T* (*cTnT*) *cre* transgene and a conditional allele of *Bmp4* that is also a hypomorph (9), revealed that *Bmp4* regulated proliferation of atrioventricular cushion mesenchyme (10).

To investigate the tissue-specific requirements for *Bmp4* signaling in the OFT, we generated a *Bmp4* conditional null allele to analyze *Bmp4* function in OFT morphogenesis directly. Inactivation of *Bmp4* in splanchnic and branchial-arch mesoderm and OFT myocardium by using the *Nkx2.5^{cre}* allele resulted in severe defects in OFT septation with AP window. Markers of aortic-sac and OFT myocardium were reduced or absent, suggesting that *Bmp4* has a role in myocardial differentiation. Interestingly, cell proliferation was up-regulated in *Bmp4* mutant OFT myocardium but reduced in cushion mesenchyme. We also found that recruitment of vascular smooth muscle to forming vessels was reduced in *Nkx2.5^{cre}; Bmp4* conditional mutant embryos. Finally, crosses of *Bmp4* conditional mutants to *Bmp7* mutant embryos uncovered a strong genetic interaction.

Materials and Methods

Whole-Mount and Section *in Situ* Hybridization. Whole-mount and section *in situ* hybridization was performed as described (11).

Casting-Dye Injection. Embryos were harvested, and the yellow casting dye (Connecticut Biological Supply, South Hampton, MA) was injected into the ventricle by using pulled glass, fixed in buffered formalin, dehydrated, and cleared in BABB (2:1 benzyl alcohol/benzyl benzoate).

LacZ Staining and Histology. Staining for LacZ and histology were performed as described (11).

Generation of the *Bmp4^{floxneo}* and *Bmp4^{null}* Alleles and Other Strains. To generate the *Bmp4^{floxneo}* allele, a targeting vector was constructed that introduced one LoxP site into an *Eco*RI site upstream of the *Bmp4* fourth exon while another LoxP site followed by a *frt* flanked *PGKneo* cassette was introduced into a downstream *Bam*HI site (see Fig. 8, which is published as supporting information on the PNAS web site). To generate the *Bmp4^{null}* allele, we crossed the *Bmp4^{floxneo}* allele to the *nestin cre* transgenic line, directing cre expression in the germline (12). The *Bmp7^{tm1}* null allele (The Jackson Laboratory) and the *prx1^{cre}* line have been described (13, 14).

Proliferation and Apoptosis. Proliferating cell nuclear antigen (PCNA) staining was performed according to the manufacturer's instructions (Zymed), and terminal deoxynucleotidyltransferase-mediated dUTP nick end labeling analysis was performed according to the manufacturer's protocol (Serologicals, Clarkston, GA).

This paper was submitted directly (Track II) to the PNAS office.

Abbreviations: OFT, outflow tract; BAA, branchial-arch artery; PT, pulmonary trunk; AP, aorto-pulmonary; SHF, secondary heart field; dpc, days postcoitum; PA, pulmonary artery; PCNA, proliferating cell nuclear antigen.

‡To whom correspondence should be addressed. E-mail: jmartin@ibt.tamushsc.edu.

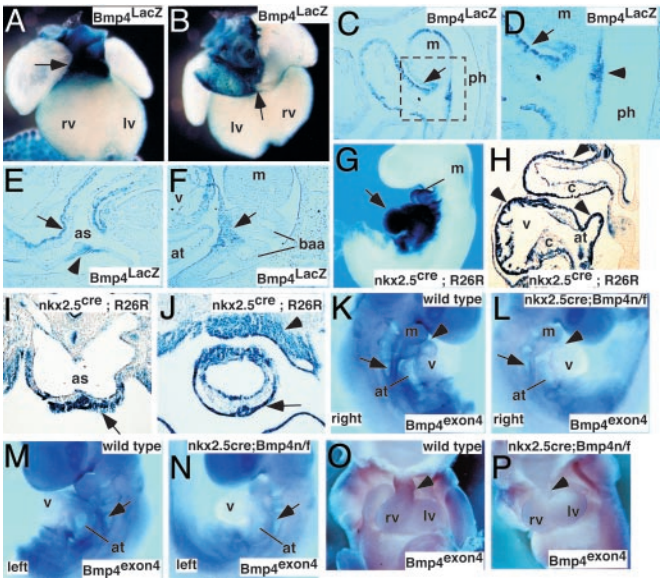

Fig. 1. *Bmp4* expression and tissue-specific inactivation in mouse embryos. (*A* and *B*) $Bmp4^{LacZ}$ expression in 10.5-dpc wild-type embryos. Ventral (*A*) and dorsal (*B*) views show *Bmp4* expression restricted to the OFT (arrow in *A*) and in the cardinal veins that drain into the right atrium (arrow in *B*). (*C–F*) Parasagittal (*C*, *D*, and *F*) and transverse (*E*) sections through 9.0-dpc mouse embryos. *D* is a magnification (×400) of the boxed area in *C*. *Bmp4* expression in OFT myocardium (arrows in *C* and *D*) and myocardium near the junction of the aortic sac and the BAA (arrow in *E*) is shown. *Bmp4* expression in the pharyngeal endoderm (arrowhead in *D* and *E*) and branchial-arch mesenchyme (arrow in *F*) is shown. (*G–J*) $Nkx2.5^{cre;}R26R$ compound mice stained for LacZ to detect cre activity at 9.5 dpc (*G* and *H*) and 10.5 dpc (*I* and *J*). Parasagittal (*H*) and coronal (*I* and *J*) sections show cre activity in OFT myocardium (arrows in *H–J*), branchial-arch mesoderm (arrowhead in *J*), and atrioventricular myocardium (arrowheads in *H*). (*K–P*) *In situ* analysis with *Bmp4* exon 4 probe at 9.0 (*K–N*) and 11.5 (*O* and *P*) dpc, comparing hybridization signal in OFT myocardium (arrowhead in *K* and *L*) and branchial-arch region (arrows in *K–N*). as, aortic sac; at, atrium; c, cushion; m, mandible; lv, left ventricle; rv, right ventricle; ph, pharynx; v, ventricle.

Results

Expression of *Bmp4* in the Branchial-Arch and Splanchnic Mesoderm and the OFT Myocardium. We examined *Bmp4* expression by using the *Bmp4* LacZ knock-in allele, $Bmp4^{LacZ}$, which had been generated (6). Whole-mount analysis and sectioning revealed that *Bmp4* was highly expressed in the OFT of the heart at 9.0 and 10.5 dpc (Fig. 1 *A–E*). *Bmp4* was detected in the coronary sinus and inferior and superior vena cava (Fig. 1*B*). *Bmp4* was expressed in OFT myocardium and in myocardium overlying the junction of the branchial-arch artery (BAA) and the aortic sac (Fig. 1 *C–E*). Expression was detected also at 9.0 dpc within mesoderm ventral to the BAAs (Fig. 1*F*). These cells have been proposed to comprise the SHF that migrates and contributes to OFT myocardium (3). Together, these data suggest that *Bmp4* functions in the formation of the OFT myocardium at early stages of its formation in the branchial arch and splanchnic mesoderm. *Bmp4* may have a role in OFT maturation by signaling to underlying conotruncal cushions. Expression in mesenchyme surrounding BAAs and in the myocardium overlying the junction between the aortic sac and the BAA suggests a function for *Bmp4* in BAA remodeling.

Inactivation of *Bmp4* in the Branchial Arch Mesenchyme and OFT Myocardium by Using the $Nkx2.5^{cre}$ Allele. To investigate *Bmp4* in the OFT, we constructed a *Bmp4* conditional null allele, the $Bmp4^{floxneo}$ allele (see *Materials and Methods* and Fig. 8). This allele of *Bmp4* contains LoxP sites surrounding exon 4, encoding the mature *Bmp4* peptide, a region of *Bmp4* that is essential for its function. Removal of exon 4 would be predicted to result in a *Bmp4* null allele.

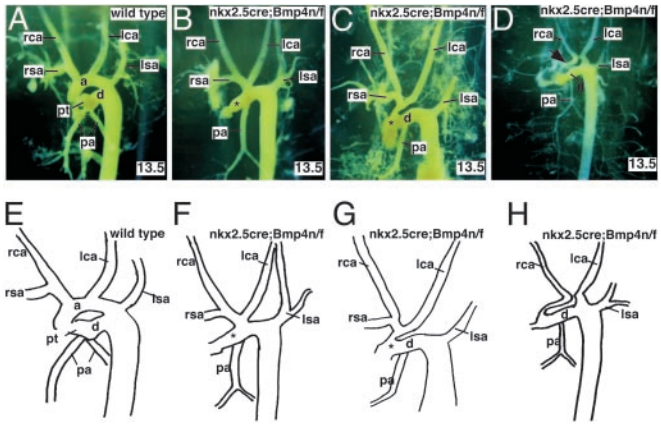

Fig. 2. Casting-dye analysis of vascular morphogenesis in $Nkx2.5^{cre}$; *Bmp4 n/f* mutant embryos. (*A–D*) Yellow casting-dye injections at 13.5 dpc, photographed in left-oblique orientation. Wild-type (*A*) and three classes of phenotypes (*B–D*) are shown. In *B* and *C*, areas of defective septation are indicated (by an asterisk), and undersized aorta (*D*) is indicated by an arrow. (*E–H*) Diagrams of wild-type and mutant dye injections from *A–D*. Each diagram is a representation of the cast image above it. a, ascending aorta; d, ductus arteriosus; lca, left carotid artery; lsa, left subclavian artery; rca, right carotid artery; rsa, right subclavian artery.

To inactivate *Bmp4* in the branchial arch and splanchnic mesoderm, as well as aortic-sac and OFT myocardium, we used the $Nkx2.5^{cre}$ knock-in allele that directs *cre* activity to these regions of the heart, the prospective SHF, and pharyngeal endoderm (ref. 15 and Fig. 1 *G–J*). The $Nkx2.5^{cre}$ allele also directs cre activity to the ventricular and atrial myocardium (Fig. 1*H*). To determine whether *Bmp4* exon 4 had been deleted in the forming hearts of $Nkx2.5^{cre}$; *Bmp4null/flox (n/f)* mutant embryos, we performed whole-mount analysis with a *Bmp4* exon 4-specific probe. At 9.0 dpc, *Bmp4* exon4 was expressed in branchial arch and splanchnic mesoderm, whereas in the $Nkx2.5^{cre}$; *Bmp4 n/f* mutant embryos, expression of *Bmp4* exon 4 was not detected (Fig. 1 *K–N*). Similarly, at 11.5 dpc, expression of *Bmp4* exon4 was absent from the OFT myocardium of $Nkx2.5^{cre}$; *Bmp4 n/f* mutant embryos, (Fig. 1 *O* and *P*). From these data, we conclude that $Nkx2.5^{cre}$; *Bmp4 n/f* embryos efficiently delete *Bmp4* exon4 in branchial-arch and splanchnic mesoderm and in the OFT myocardium.

***Bmp4* Is Required for Normal Septation of the OFT and BAA Remodeling.** Most $Nkx2.5^{cre}$; *Bmp4 n/f* mutant embryos died by 13.5 dpc, although there was a range of lethality, with an occasional $Nkx2.5^{cre}$; *Bmp4 n/f* mutant embryo surviving until 18.5 dpc. The variability in expressivity of the $Nkx2.5^{cre}$; *Bmp4 n/f* mutant phenotype most likely results from variability of cre activity (data not shown). At time points before lethality, we noted that the $Nkx2.5^{cre}$; *Bmp4 n/f* mutant embryos had peripheral edema that was often associated with a pericardial effusion, suggesting that embryonic lethality was secondary to heart failure (data not shown).

We performed casting-dye injections at two developmental time points to visualize the OFT and BAAs in $Nkx2.5^{cre}$; *Bmp4 n/f* mutant embryos. At 12.0 dpc, both wild-type and $Nkx2.5^{cre}$; *Bmp4 n/f* mutant embryos had well formed BAAs, revealing that the initial assembly of the endothelial tubes was intact in the $Nkx2.5^{cre}$; *Bmp4 n/f* mutant embryos (data not shown). In contrast, at 13.5 dpc, after remodeling of the OFT and BAAs, the $Nkx2.5^{cre}$; *Bmp4 n/f* mutant embryos had severe defects in the architecture of the BAAs (Fig. 2 *A–D*).

In wild-type embryos, the right brachiocephalic, left carotid, and left subclavian arteries branch directly from the ascending aorta (Fig. 2. *A* and *E*). In $Nkx2.5^{cre}$; *Bmp4 n/f* mutant embryos, the left carotid branched either from the right brachiocephalic artery in the most severe embryos or directly from the aorta in more mildly

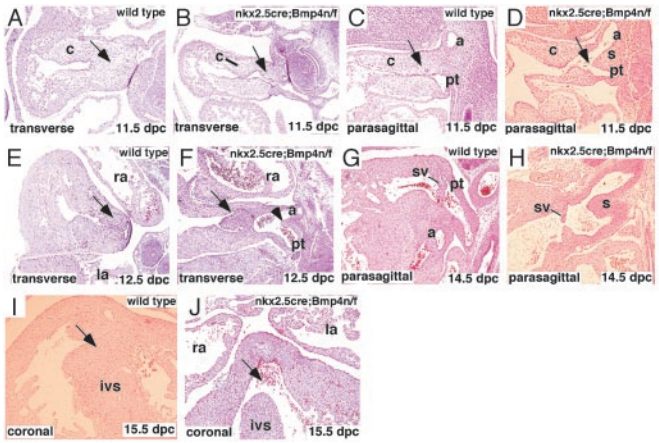

Fig. 3. Histologic analysis of *Nkx2.5^{cre}; Bmp4 n/f* mutant embryos. (*A–D*) Transverse (*A* and *B*) and parasagittal (*C* and *D*) sections through the OFT of wild-type (*A* and *C*) and *Bmp4* conditional mutant (*B* and *D*) embryos at 11.5 dpc. Distal septal cushions are reduced in *Bmp4* mutants (compare arrows in *A–D*). Communication between PT and aorta is evident (arrow in *D*). (*E* and *F*) Transverse sections of wild-type (*E*) and *Bmp4* mutant (*F*) at 12.5 dpc reveal communication between PT and aorta (arrowhead in *F*) and abnormal cushions (compare arrows in *E* and *F*). (*G* and *H*) Parasagittal sections reveal septated and remodeled OFT septum in wild-type (G) and AP window in mutant with valve hypoplasia in mutants (*H*). (*I* and *J*) The ventricular septum has fused in the wild-type 15.5-dpc embryo (arrow in *I*) but a membranous ventricular septal defect in mutant (arrow in *J*). a, aorta; c, cushion; ivs, interventricular septum; left atrium; ra, right atrium; s, AP septum; sv, semilunar valve.

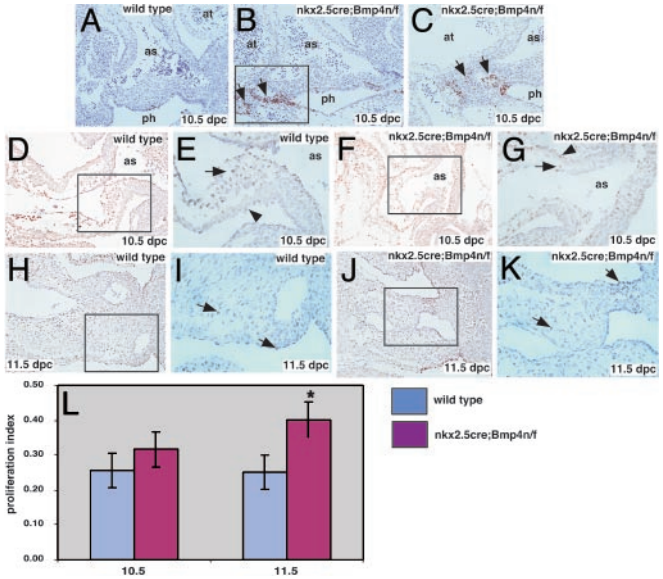

Fig. 4. Defects in proliferation and apoptosis in *Nkx2.5^{cre}; Bmp4 n/f* mutant embryos. (*A–C*) Terminal deoxynucleotidyltransferase-mediated dUTP nick end labeling in transverse sections of 10.5-dpc embryos. Stages and genotypes are labeled. Arrows in *B* indicate areas of up-regulated apoptosis in the *Nkx2.5^{cre}; Bmp4 n/f* mutants in both mesenchyme and pharyngeal endoderm. *C* is a higher magnification (×400) of the boxed area in *B*. (*D–K*) PCNA staining at two stages: 10.5 (*D–G*) and 11.5 (*H–K*) dpc. The data for the OFT myocardium are also presented in *L*. At 10.5 dpc, the *Nkx2.5^{cre}; Bmp4 n/f* mutants have severely reduced OFT cushions with fewer PCNA-positive cells (compare arrows in *E* and *G*). The 10.5-dpc OFT myocardium has similar numbers of PCNA-positive cells in wild-type and *Nkx2.5^{cre}; Bmp4 n/f* mutants (compare arrowheads in *E* and *G*). At 11.5 dpc, the *Nkx2.5^{cre}; Bmp4 n/f* mutant OFT cushion (*J* and *K*) has enlarged but lags behind wild type (*H* and *I*). (*L*) Proliferative index in OFT myocardium of wild-type and *Nkx2.5^{cre}; Bmp4 n/f* mutants at two stages. as, aortic sac; at, atrium; ph, pharynx. At 11.5 dpc, the mutant has a statistically significant increase in proliferation. *, $P < 0.05$ (χ^2 test).

affected embryos (Fig. 2). In all of the mildly affected embryos, there was an aortic interruption between the left carotid and the left subclavian, known as a type B interruption (Fig. 2. *C* and *G*) and (16). In all *Bmp4* mutant embryos, only one pulmonary artery (PA), originating from the ductus arteriosus in the injected embryos, was identified (Fig. 2. *B–D* and *F–H*). The origin of the second PA is unclear, although, in human patients, the PA is known to originate from many places, including the right ventricle (17).

Defects were also observed in septation of the OFT. The most severe defect, observed in two embryos, was persistent truncus arteriosus, although we cannot rule out the alternative classification of total AP window (17, 18) (Fig. 2 *B* and *F*). The most common OFT anomaly in *Nkx2.5^{cre}; Bmp4 n/f* mutant embryos was a proximal, AP window in which the most proximal aspect of the OFT septum failed to form (17). This defect was found in the majority of *Nkx2.5^{cre}; Bmp4 n/f* mutant embryos (Fig. 2 *C* and *G*). The final abnormality, observed in three *Nkx2.5^{cre}; Bmp4 n/f* mutants, was failure of proximal septation with unequal sizes of the PT and ascending aorta (Fig. 2 *D* and *H*).

Microscopic Analysis Revealed Defects in Conotruncal and Atrioventricular Septation in *Nkx2.5^{cre}; Bmp4 n/f* Mutants. Sections of embryos revealed that at 11.5 dpc, septation within the distal OFT of wild-type embryos was progressing, whereas in *Nkx2.5^{cre}; Bmp4 n/f* mutant embryos, cushion growth was delayed (Fig. 3 *A–D*). At 11.5 dpc, the separation of the aorta from the PT had initiated in wild-type embryos, but in *Nkx2.5^{cre}; Bmp4 n/f* mutant embryos, the distal OFT remained unseptated with hypoplastic cushions (Fig. 3 *C* and *D*). At 12.5 dpc, the distal septum of wild-type embryos was extensive, whereas in the mutant embryos, the communication between the aorta and PT was clearly visible (Fig. 3 *E* and *F*). By 14.5 dpc, the OFT had undergone substantial remodeling and septation in wild-type embryos, but in the *Bmp4* mutant, septation failed to progress, resulting in the proximal AP window defect that was also observed in the casting-dye injections. Moreover, the semilunar valves in the mutant were clearly hypoplastic in the 14.5-dpc embryos when compared with wild type (Fig. 3 *G* and *H*).

We also observed ventricular septal defects in all mutant embryos (Fig. 3 *I* and *J*). Histologic analysis showed that the ventricular septal defect likely results from a deficiency in the contruncal mesenchyme, which is in proximity to the AV-cushion mesenchyme and is thought to be important for septation and for walling off the left AV canal from the right ventricle (19). Together with the casting-dye data, these data show that *Bmp4* function is necessary for growth of the conotruncal cushions and OFT septation, as well as BAA remodeling. These data also suggest that *Bmp4* has a more important function in proximal OFT septation.

***Bmp4* Regulates Cellular Proliferation in the OFT.** To investigate the hypothesis that *Bmp4* regulated proliferation and/or apoptosis in the forming OFT, we used terminal deoxynucleotidyltransferase-mediated dUTP nick end labeling studies on serial sections. These studies revealed a modest up-regulation of apoptotic cells in the pharyngeal endoderm and surrounding mesenchyme in proximity to the aortic sac of *Nkx2.5^{cre}; Bmp4 n/f* mutant embryos (Fig. 4 *A–C*).

PCNA immunostaining experiments revealed that at 10.5 dpc, cell proliferation in the *Nkx2.5^{cre}; Bmp4 n/f* mutant OFT cushions was severely reduced. Fewer proliferating cells were found in the hypoplastic cushions of the *Nkx2.5^{cre};Bmp4 n/f* mutants (Fig. 4 *D–G*). At 11.5 dpc, when more *Bmp4* mutant OFT-cushion mesenchyme had formed, cell counting of PCNA-positive cells revealed a significant reduction in the number of proliferating cells in the mutant embryos. At 11.5 dpc, the proliferative index of OFT cushion mesenchyme in wild-type embryos was 43.3 ± 1.0%,

DEVELOPMENTAL BIOLOGY

whereas in the *Bmp4* mutant the proliferative index was 33.6 ± 2.7% ($P < 0.05$, Student's *t* test).

We also noted that the number of PCNA-positive cells in the OFT myocardium of *Nkx2.5^{cre}; Bmp4 n/f* mutants was greater than in the wild-type controls. At both 10.5 and 11.5 dpc, the proliferative index in *Nkx2.5^{cre}; Bmp4 n/f* mutants was greater than in the wild-type controls, although this difference was statistically significant only at 11.5 dpc (Fig. 4 *H–L*). Taken together, these data reveal that *Bmp4* functions in both the regulation of apoptosis and proliferation in OFT development. The role of *Bmp4* in regulation of apoptosis is likely a minor one with regard to OFT morphogenesis because elevated apoptosis was observed in only a few sections of our serial section analysis. In contrast, regulation of proliferation, with an interesting difference between the myocardium and mesenchyme, appears to be a major function for *Bmp4* in the OFT. *Bmp4* promotes proliferation of cushion mesenchyme and concurrently represses cell proliferation in the OFT myocardium.

***HAND* Genes are Down-Regulated in the Aortic-Sac Myocardium of *Nkx2.5^{cre}; Bmp4 n/f* Mutant Embryos.** We next examined markers of the aortic-sac and OFT myocardium. Expression of the basic helix–loop–helix genes, *eHAND* and *dHAND*, was severely reduced in the *Nkx2.5^{cre}; Bmp4 n/f* mutant embryos (Fig. 5 *A*, *B*, *E*, and *F*). Sections through wild-type and *Nkx2.5^{cre}; Bmp4 n/f* mutant embryos revealed that *eHAND* expression was reduced or absent in the myocardium of the aortic sac and posterior pericardial wall (Fig. 5 *C* and *D*), whereas *dHAND* was reduced in the aortic-sac myocardium (Fig. 5 *G* and *H*). Expression of *eHAND* was maintained at normal levels in the left ventricle of the *Nkx2.5^{cre}; Bmp4 n/f* mutant embryos (Fig. 5 *A* and *B*). Expression of *sema3c* and *pitx2* was also reduced in the OFT myocardium of 11.5-dpc mutant embryos (Fig. 5 *I–L*). In contrast, *Bmp7*, which is normally expressed in the OFT and right ventricular myocardium, was expanded in the OFT of *Nkx2.5^{cre}; Bmp4 n/f* mutant embryos (Fig. 5 *M* and *N*). Expression of LacZ from the *Bmp4^{LacZ}* allele in *Nkx2.5^{cre}; Bmp4 n/f* mutants was intact, suggesting that anterior myocardium moved correctly into the OFT. This observation also reveals that *Nkx2.5^{cre}; Bmp4 n/f* mutant cells had maintained their fate as *Bmp4* expressing cells (Fig. 5 *O–R*). These data suggest that *Bmp4* signaling functions in differentiation of the aortic-sac and OFT myocardium.

Because defects in cardiac neural crest may also result in similar phenotypes of defective vascular remodeling, we analyzed markers of cardiac neural crest in *Nkx2.5^{cre}; Bmp4 n/f* mutant embryos. Expression of *crabp1*, *ap2* and *hoxa2* was detected at normal levels in the migrating neural crest of *Nkx2.5^{cre}*; *Bmp4 n/f* mutant embryos. These data suggested that the initial migration of the cardiac neural crest was intact in the *Nkx2.5^{cre}; Bmp4 n/f* mutant embryos (Fig. 5 *S* and *T*, and data not shown).

***Bmp4* Signaling Is Required to Recruit Vascular Smooth Muscle to Forming BAAs and the Conotruncal Region of the Heart.** One possible explanation for defective vascular remodeling in *Nkx2.5^{cre}; Bmp4 n/f* mutant embryos was a deficiency in smooth-muscle recruitment to the formed endothelial tubes in the *Nkx2.5^{cre}; Bmp4 n/f* mutant embryos. We used the *sm22^{LacZ}* transgene, which marks vascular smooth muscle (20), to visualize smooth muscle in *Nkx2.5^{cre}; Bmp4 n/f* mutant embryos. Because smooth muscle is a neural-crest derivative, this experiment would also determine whether neural-crest development was defective in the *Nkx2.5^{cre}; Bmp4 n/f* mutants (21). At 11.5 dpc, recruitment of smooth-muscle cells to the BAAs was detected in the wild-type embryos, but in *Nkx2.5^{cre}; Bmp4 n/f* mutant embryos fewer smooth-muscle cells were observed surrounding the BAAs (Fig. 6 *A–D*).

By 12.5 dpc, the difference in smooth-muscle recruitment was exacerbated in the *Nkx2.5^{cre}; Bmp4 n/f* mutant embryos. Fewer LacZ-positive cells were found in the OFT, as well as, the BAAs of *Nkx2.5^{cre}; Bmp4 n/f* mutant embryos. *Nkx2.5^{cre}*; *Bmp4 n/f* mutants also had fewer LacZ-positive cells in the proximal OFT and ventricles (Fig. 6 *E–H*). Sections revealed that in wild-type embryos, LacZ-positive smooth-muscle cells contributed to the proximal OFT, whereas in *Nkx2.5^{cre}*; *Bmp4 n/f* mutants, LacZ-positive cells were only detected distally (Fig. 6 *I–L*). Taken together, these data suggest that *Bmp4* signaling has a central role in stabilization of forming vessels by promoting the recruitment or differentiation of vascular smooth muscle and supports the notion that neural-crest derivatives fail to expand in the *Bmp4* mutants.

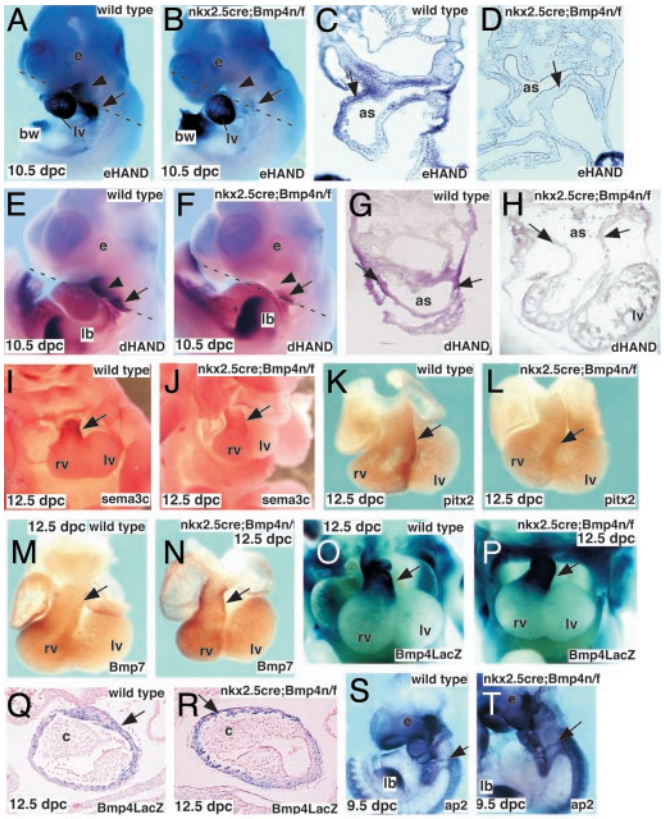

Fig. 5. Defects in markers of aortic sac and OFT myocardium in *Nkx2.5^{cre}; Bmp4 n/f* mutant embryos. (*A–H*) *In situ* analysis with *eHAND* (A–D) and *dHAND* (E–H) probes (*A*, *B*, *E*, and *F*) and transverse sections (*C*, *D*, *G*, and *H*). Plane of section is indicated by dotted line (*A*, *B*, *E*, and *F*). Expression is reduced in the mutant aortic sac (arrow in *A–H*) and in branchial arch (arrowhead in *A*, *B*, *E*, and *F*). The body wall that expresses *eHAND* has been partially removed (*A* and *B*). Expression of *dHAND* in the branchial pouches is reduced (*E* and *F*). (*I–N*) *In situ* analysis with *sema3c* (*I* and *J*), *pitx2* (*K* and *L*), and *Bmp7* (*M* and *N*) probes. Signal is indicated by arrows. (*O–R*) LacZ staining directed by *Bmp4 LacZ*. Whole-mount LacZ staining reveals LacZ-positive cells in OFT of wild-type and *Bmp4* mutant embryos (arrows). Coronal sections (*Q* and *R*) reveal LacZ-positive cells in OFT myocardium (arrows). (*S* and *T*) *In situ* analysis with *ap2* probe on 9.5-dpc wild-type (*S*) and *Bmp4* mutant (*T*) embryos. Arrows indicate the migrating cardiac neural-crest cells. as, aortic sac; bw, body wall; c, cushions; e, eye; rv, right ventricle; lb, limb bud; lv, left ventricle.

***Bmp7* Cooperates with *Bmp4* in Morphogenesis of the OFT.** The *Nkx2.5^{cre}; Bmp4 n/f* mutant embryos had a delay in formation of the OFT cushions, suggesting that other Bmp family members functioned in cushion morphogenesis. Moreover, in the *Nkx2.5^{cre}; Bmp4 n/f* mutant embryos we found that expression of *Bmp7* was up-regulated in OFT myocardium. To test the hypothesis that *Bmp7* had overlapping function with *Bmp4* in OFT morphogenesis, we generated compound *Bmp4;Bmp7* mutant embryos.

The *prx1^{cre}* transgene directs low levels of cre activity to the OFT myocardium (Fig. 7 *A* and *B*). As a result of low cre activity in OFT myocardium, the *prx1^{cre};Bmp4 n/f* embryos have no obvious OFT defect (Fig. 7 *C* and *D*). However, because *Bmp4* dosage is

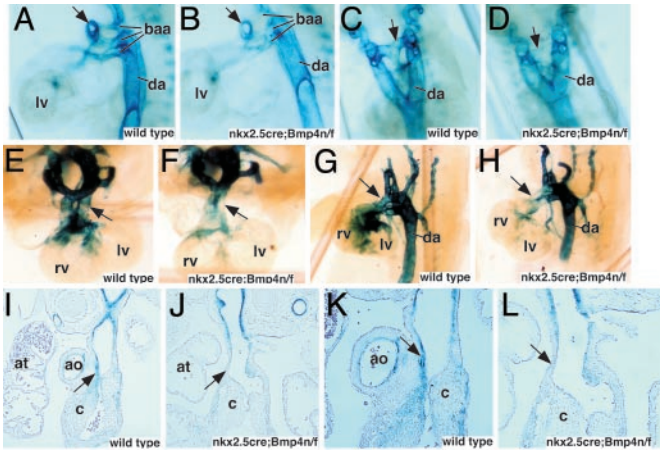

Fig. 6. Smooth-muscle recruitment is defective in the absence of *Bmp4* signaling. (*A–D*) $sm22^{LacZ}$ expression at 10.5 dpc expression in aortic sac is reduced in mutant oblique lateral (*A* and *B*) and frontal (*C* and *D*) views. Compare arrows in *A* and *B* as well as in *C* and *D*. (*E–H*). Whole-mount view of $sm22^{LacZ}$ expression at 12.5 dpc in wild-type and *Bmp4* mutant embryos. Arrows indicate areas of reduced contribution of LacZ-positive cells in mutant. (*I–L*) Sections through 12.5-dpc embryos. Arrows indicate areas of reduced LacZ staining in the *Bmp4* mutant in whole-mount views and sections. ao, aorta; at, atrium; c, cushion; da, dorsal aorta; rv, right ventricle; lv, left ventricle.

reduced, these embryos provide a sensitized background to test for a genetic interaction with *Bmp7* in the OFT myocardium (Fig. 7 *E* and *F*). Although the $Bmp7^{tm1-/-}$ embryos had normal formation of the OFT cushions, the $prx1^{cre}$*; Bmp4 n/f;* $Bmp7^{tm1+/-}$ mice had slightly hypoplastic OFT cushions (Fig. 7 *D–F*). Moreover, the $prx1^{cre}$*; Bmp4 n/f;* $Bmp7^{tm1-/-}$ embryos had severe defects in OFT morphogenesis in which OFT cushions were severely reduced and the OFT was shortened (Fig. 7*G*). These data strongly suggest that *Bmp4* and *Bmp7* have overlapping functions in OFT morphogenesis.

Discussion

Our data reveal that *Bmp4* function is important for differentiation of OFT myocardium and for expansion of the OFT-cushion mesenchyme. Our results also show that *Bmp4* is required for recruitment of vascular smooth muscle to forming BAAs and, therefore, provide insight into these events. Last, our data uncover a strong genetic interaction between *Bmp4* and *Bmp7*, suggesting that these genes have overlapping functions in the OFT.

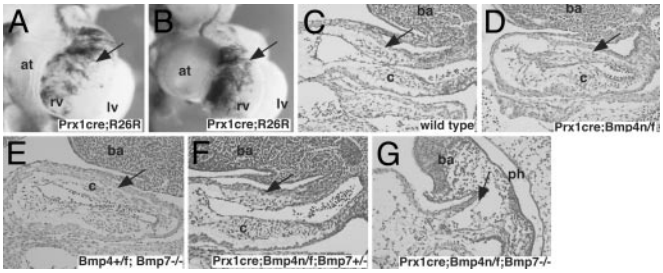

Fig. 7. Coordinate regulation of OFT septation by *Bmp4* and *Bmp7*. (*A* and *B*) LacZ staining of $prx1^{cre}$*; rosa 26 reporter (R26R)* compound heterozygotes at 10.5 dpc in frontal (*A*) and right-oblique (*B*) views. LacZ staining identifies cells that have cre activity (arrow). (*C–G*) Parasaggital sections (hematoxylin/eosin) of 10.5-dpc compound *Bmp4; Bmp7* mutant and controls. Area of abnormality in $prx1^{cre}$*; Bmp4 n/f;* $Bmp7^{tm1-/-}$ embryos and corresponding area in controls (arrows). at, atrium; ba, branchial arch; c, cushion; rv, right ventricle; lv, left ventricle.

***Bmp4* Functions to Recruit Vascular Smooth Muscle to the BAAs.** Our results uncover a role for *Bmp4* in the development of the BAAs. We propose that the defect involves a delay in recruitment of neural crest-derived vascular smooth muscle to the formed endothelial tubes of the BAAs. Formation of the BAAs, and later remodeling into adult aortic-arch arteries, involves paracrine signaling (22). The forming BAA endothelial tubes are located within the branchial-arch mesenchyme in close proximity to surface ectoderm and the endoderm of the branchial pouches and pharynx. Moreover, signaling from endothelium to mesenchyme functions in the recruitment of supporting cells, such as smooth-muscle precursors and pericytes, which are important for vessel stabilization (22). The $Nkx2.5^{cre}$ knock-in allele directs cre activity in both the branchial-arch mesenchyme, as well as the pharyngeal endoderm. This finding suggests that *Bmp4* may cooperate with endothelial-derived signals in vascular smooth-muscle development. In the future, it will be important to dissect the exact source of *Bmp4* that is important for BAA development.

In vasculature remodeling, there is a local disruption of the interaction between endothelium and supporting cells. This disruption results in regression of the endothelium that likely involves programmed cell death (23). Cell-ablation studies in chick embryos and loss-of-function experiments performed in mice have defined a role for the cardiac crest in maintaining the integrity of the BAAs (21, 24). Moreover, recent fate-mapping experiments using the *wnt1 cre* and *rosa 26 reporter* mice confirmed the importance of the cardiac crest in mouse BAA formation (2).

Our results show that recruitment of smooth muscle to the BAAs is reduced in $Nkx2.5^{cre}$*; Bmp4 n/f* mutants. Therefore, *Bmp4* may be necessary for migration, local proliferation, survival, or differentiation of the vascular smooth muscle. Although we found evidence for elevated apoptosis in the branchial-arch mesenchyme of $Nkx2.5^{cre}$*; Bmp4 n/f*, the apoptosis was very restricted and unlikely to be the mechanism for the severe BAA phenotype. Moreover, because we did not detect a major proliferation defect in *Bmp4* mutant branchial arch mesenchyme, we favor the hypothesis that *Bmp4* is required for differentiation of neural crest-derived mesenchyme into vascular smooth muscle.

The Function of *Bmp4* in OFT Septation. There is disagreement regarding the relative contributions of the conotruncal cushions and AP septum in the septation process (19). Our work reveals that *Bmp4* provides a signal to the conotruncal cushions that regulates cushion growth. Although cushions still form in the *Bmp4* mutant OFT as a result of the overlapping function of *Bmp7* (see below), there is a severe proliferation defect in the hypoplastic *Bmp4* mutant OFT cushions. Our marker analysis suggested that the initial migration of the cardiac crest was intact in the $Nkx2.5^{cre}$*; Bmp4 n/f* mutants but that neural crest-derived smooth-muscle cells, marked by $sm22^{LacZ}$, failed to populate the proximal OFT of *Bmp4* mutant embryos. The deficiency in neural crest-derived smooth muscle suggests that the cardiac neural crest that normally contributes to OFT cushions and the AP septum is also reduced in the proximal OFT of $Nkx2.5^{cre}$*; Bmp4 n/f* mutant embryos.

We found that cell proliferation was reduced in the cushion mesenchyme of $Nkx2.5^{cre}$*; Bmp4 n/f* mutants. One possibility is that *Bmp4* has a direct role in promoting local proliferation of neural-crest cells after they have reached the OFT. *Bmp4* might also be important for promoting migration of neural crest destined for the proximal OFT. In support of this notion, overexpression of *noggin* in chick embryos suggested that *Bmp* signaling was important for both the migration of cardiac neural crest into the OFT and the proliferation of cushion mesenchyme (8). However, because OFT cushions derive from both endocardium and cardiac neural crest, it is also possible that *Bmp4* signals to the endocardium and promotes the mesenchymal transformation important to OFT-cushion development.

Although further experiments are required to distinguish be-

DEVELOPMENTAL BIOLOGY

tween these possibilities, our data show that *Bmp4* promotes expansion of incoming OFT neural crest.

Our results support the proposal that there are distinct pathways regulating septation of the proximal and distal OFT (7). For example, high levels of *Bmp*-signaling may be required for proximal OFT septation. In the *Nkx2.5^{cre}; Bmp4 n/f* mutant embryos, total *Bmp* signaling may be reduced sufficiently to interfere with proximal, but not distal, septation.

Our data expand on these ideas by showing that the total level of *Bmp4* and *Bmp7* expression are important in OFT septation. *Bmp7* expression was up-regulated in the *Nkx2.5^{cre}; Bmp4 n/f* mutant OFT suggesting a regulatory mechanism controlling total *Bmp* levels in OFT myocardium. The severe OFT phenotype of *prx1^{cre};Bmp4 n/f; Bmp7$^{tm1-/-}$* mutant embryos revealed that *Bmp4* and *Bmp7* have overlapping functions in OFT-cushion morphogenesis. It has also been observed that *Bmp7* cooperates with *Bmp6* in OFT development (25). Together, these data suggest that total levels of *Bmp4* and *Bmp7* regulate cushion development and support the hypothesis that proximo-distal patterning of OFT cushions is regulated by total levels of *Bmp* signaling.

Bmp4 and the Differentiation of the OFT Myocardium and the Prospective SHF. Experiments performed in chick embryos have implicated a *Bmp2*- mediated pathway in specification of the branchial arch and splanchnic mesoderm that will populate the OFT myocardium (26). Our experiments suggest that, in the mouse, this *Bmp*-signaling function has been partly assumed by *Bmp4*. The invasion of cells from this SHF, complete by 9.5 dpc in the mouse, may be important for lengthening and arterialization of the OFT (3).

Our data showing *Bmp4^{LacZ}* expression in the OFT of *Bmp4* mutant embryos suggest that cells from the branchial arch and splanchnic mesoderm still migrate into the OFT in the absence of *Bmp4*. Rather, *Bmp4* functions in the final differentiation of the myocardium as shown by reduction in expression of OFT myocardial markers. Moreover, along with defective OFT myocardial differentiation, we observed excessive proliferation in myocardial precursors of *Nkx2.5^{cre}; Bmp4 n/f* mutants. This observation suggests that the function of *Bmp4* in OFT myocardium (to promote differentiation) is distinct from its role in the OFT-cushion mesenchyme, where it is required for cellular expansion. It will be important to determine the underlying molecular mechanisms responsible for the different roles of *Bmp4* in the OFT.

Bmp Signaling and the dHAND and eHAND Genes. Although further analysis of regulatory elements are necessary, our data support the notion that the *dHAND* and *eHAND* genes are downstream of *Bmp4* signaling. *eHAND* expression is also regulated by Bmp signaling in *Xenopus* embryos and *dHAND* has been shown to be a target of Bmp signaling in neuronal development (27, 28). The vascular phenotype of the *dHAND* null embryos, more severe than the *Bmp4* mutant embryos, is consistent with a down-regulation of *dHAND* and *eHAND* expression in the *Bmp4* mutants (29). It is interesting to note that *dHAND* regulation is complex and likely involves many input signals, including the *endothelin* pathway. Mice that are mutant for components of the *endothelin* signaling pathway have defects in BAA remodeling, raising the possibility that *Bmp* and *endothelin* signaling may interact in BAA development (30).

Comparison with Other Cardiac-Specific _Bmp4_ Conditional Mutants. It is interesting to note that there are difference between our data and the data presented in the work describing the conditional inactivation of *Bmp4* by using the *rat cardiac troponin T* (*cTnT*) *cre* transgene, which reported severe atrioventricular canal defects and only mild OFT abnormalities (10). This work contrasts with the *Nkx2.5^{cre}; Bmp4 n/f* mutants that had only a mild membranous ventricular septal defect but more severe OFT defects. It is likely that the *cTnT* cre transgenic driver used by Jiao *et al.* (10) directs relatively low levels of cre activity in the OFT myocardium (see Fig. 2 *c–e* in ref. 10).

With regard to the more severe AV canal phenotype observed in the *cTnT cre; Bmp4* mutants, it is important to note that the conditional *Bmp4* null allele used by Jiao *et al.* (10) is a hypomorph, as reported by the same group (9). *Bmp4* is also known to be expressed in lateral-plate mesoderm at early embryonic stages and has a role in left right asymmetry (31). Because the mice reported by Jiao *et al.* (10) are hypomorphs, they have reduced levels of *Bmp4* in lateral-plate mesoderm and other areas where *Bmp4* is expressed. Thus, it is possible that the more severe AV canal phenotype observed by Jiao *et al.* (10) results from the hypomorphic *Bmp4* allele that has early defects in *Bmp4* expression before cardiac organogenesis.

We thank A. Bradley, P. Soriano, and R. Behringer for reagents; B. Hogan, J Epstein, E. Olson, D. Srivistava, P. Chambon, and T. Gridley for *in situ* probes; B. Hogan and Y. Furuta for the *Bmp4 ^{LacZ}* allele; and E. Olson for the sm22 LacZ transgenic line. This work was supported by National Institutes of Dental and Craniofacial Research Grants 2R01DE/HD12324-06 and R01 DE013509 (to J.F.M.) and National Institutes of Health Grants R01 HL50422 and P01 HL49953 (to R.J.S.).

1. Olson, E. N. & Schneider, M. D. (2003) *Genes Dev.* **17,** 1937–1956.
2. Jiang, X., Rowitch, D. H., Soriano, P., McMahon, A. P. & Sucov, H. M. (2000) *Development (Cambridge, U.K.)* **127,** 1607–1616.
3. Kelly, R. G. & Buckingham, M. E. (2002) *Trends Genet.* **18,** 210–216.
4. Hogan, B. L. (1996) *Curr. Opin. Genet. Dev.* **6,** 432–438.
5. Abdelwahid, E., Rice, D., Pelliniemi, L. J. & Jokinen, E. (2001) *Cell Tissue Res.* **305,** 67–78.
6. Lawson, K. A., Dunn, N. R., Roelen, B. A., Zeinstra, L. M., Davis, A. M., Wright, C. V., Korving, J. P. & Hogan, B. L. (1999) *Genes Dev.* **13,** 424–436.
7. Delot, E. C., Bahamonde, M. E., Zhao, M. & Lyons, K. M. (2003) *Development (Cambridge, U.K.)* **130,** 209–220.
8. Allen, S. P., Bogardi, J. P., Barlow, A. J., Mir, S. A., Qayyum, S. R., Verbeek, F. J., Anderson, R. H., Francis-West, P. H., Brown, N. A. & Richardson, M. K. (2001) *Dev. Biol.* **235,** 98–109.
9. Kulessa, H. & Hogan, B. L. (2002) *Genesis (New York)* **32,** 66–68.
10. Jiao, K., Kulessa, H., Tompkins, K., Zhou, Y., Batts, L., Baldwin, H. S. & Hogan, B. L. (2003) *Genes Dev.* **17,** 2362–2367.
11. Lu, M. F., Pressman, C., Dyer, R., Johnson, R. L. & Martin, J. F. (1999) *Nature* **401,** 276–278.
12. Trumpp, A., Depew, M. J., Rubenstein, J. L., Bishop, J. M. & Martin, G. R. (1999) *Genes Dev.* **13,** 3136–3148.
13. Luo, G., Hofmann, C., Bronckers, A. L., Sohocki, M., Bradley, A. & Karsenty, G. (1995) *Genes Dev.* **9,** 2808–2820.
14. Logan, M., Martin, J. F., Nagy, A., Lobe, C., Olson, E. N. & Tabin, C. J. (2002) *Genesis (New York)* **33,** 77–80.
15. Moses, K. A., De Mayo, F., Braun, R. M., Reecy, J. L. & Schwartz, R. J. (2001) *Genesis (New York)* **31,** 176–180.
16. Backer, C. L. & Mavroudis, C. (2000) *Ann. Thorac. Surg.* **69,** S298–S307.
17. Jacobs, J. P., Quintessenza, J. A., Gaynor, J. W., Burke, R. P. & Mavroudis, C. (2000) *Ann. Thorac. Surg.* **69,** S44–S49.
18. Jacobs, M. L. (2000) *Ann. Thorac. Surg.* **69,** S50–S55.
19. Webb, S., Qayyum, S. R., Anderson, R. H., Lamers, W. H. & Richardson, M. K. (2003) *J. Anat.* **202,** 327–342.
20. Li, L., Miano, J. M., Cserjesi, P. & Olson, E. N. (1996) *Circ. Res.* **78,** 188–195.
21. Etchevers, H. C., Vincent, C., Le Douarin, N. M. & Couly, G. F. (2001) *Development (Cambridge, U.K.)* **128,** 1059–1068.
22. Hanahan, D. (1997) *Science* **277,** 48–50.
23. Meeson, A. P., Argilla, M., Ko, K., Witte, L. & Lang, R. A. (1999) *Development (Cambridge, U.K.)* **126,** 1407–1415.
24. Brown, C. B., Feiner, L., Lu, M. M., Li, J., Ma, X., Webber, A. L., Jia, L., Raper, J. A. & Epstein, J. A. (2001) *Development (Cambridge, U.K.)* **128,** 3071–3080.
25. Kim, R. Y., Robertson, E. J. & Solloway, M. J. (2001) *Dev. Biol.* **235,** 449–466.
26. Waldo, K. L., Kumiski, D. H., Wallis, K. T., Stadt, H. A., Hutson, M. R., Platt, D. H. & Kirby, M. L. (2001) *Development (Cambridge, U.K.)* **128,** 3179–3188.
27. Sparrow, D. B., Kotecha, S., Towers, N. & Mohun, T. J. (1998) *Mech. Dev.* **71,** 151–163.
28. Howard, M. J., Stanke, M., Schneider, C., Wu, X. & Rohrer, H. (2000) *Development (Cambridge, U.K.)* **127,** 4073–4081.
29. Srivastava, D., Thomas, T., Lin, Q., Kirby, M. L., Brown, D. & Olson, E. N. (1997) *Nat. Genet.* **16,** 154–160.
30. Yanagisawa, H., Hammer, R. E., Richardson, J. A., Williams, S. C., Clouthier, D. E. & Yanagisawa, M. (1998) *J. Clin. Invest.* **102,** 22–33.
31. Fujiwara, T., Dehart, D. B., Sulik, K. K. & Hogan, B. L. (2002) *Development (Cambridge, U.K.)* **129,** 4685–4696.